JOURNAL OF MATERIALS SCIENCE 26 (1991) 4534–4540

Monitoring thermal shock of alumina and zirconia-toughened alumina by acoustic techniques

I. THOMPSON, R. D. RAWLINGS
Department of Materials, Imperial College of Science, Technology and Medicine, Prince Consort Road, London SW7 2BP, UK

Acoustic emission (AE) and acousto-ultrasonics (AU) have been employed to monitor the thermally induced damage which occurs when alumina and zirconia-toughened alumina ceramics are quenched from elevated temperatures into aqueous solutions. The AE and AU parameters were correlated with the microcracking and the strength degradation associated with the thermal shock treatments.

1. Introduction

The major limitation of employing many engineering ceramics in the more stringent service environments is their poor toughness, thermal shock resistance and reliability. The situation is exacerbated by the absence of any standard non-destructive test (NDT) methods suitable for the quality control of mass produced ceramics or for the detection of degradation which may occur in service.

Two acoustic NDT methods may be applicable to ceramics. The first of these, acoustic emission (AE), is simply the monitoring of the stress waves generated by a dynamic process occurring within, or on the surface of, a material by means of a sensitive transducer, usually of the piezoelectric type. The dynamic process of most interest as far as ceramics are concerned is the growth of microcracks and, indeed, AE has been successfully used to monitor microcracking during mechanical testing [1, 2] and thermal shock treatments [3]. It should be noted that AE can only detect active defects, i.e. growing microcracks, and is therefore suitable for the continuous monitoring of damage occurring during production or service but will not detect flaws in any post-production or post-service assessment of a component which is not stressed.

On the other hand the second technique, acousto-ultrasonics (AU) is capable of post-production and post-service testing. In AU, stress waves are introduced into the component under examination by means of a pulser and, after travelling through the component, the waves are detected by another transducer. The signals from the transducer are analysed in a similar manner to that employed in AE. Thus AU monitoring assesses the general condition of the volume of material between the pulser and the receiving transducer and does not attempt to size and locate individual flaws. It follows that AU may be particularly appropriate for ND testing of ceramics as the defects are usually small, numerous and dispersed; it has been shown to be sensitive to the degree of crystallization of a glass-ceramic [4] and to the percentage porosity in sintered glass and carbon-bonded carbon fibre composites [5].

This paper reports the results of a study of the employment of these two acoustic techniques in an investigation of the thermal shock resistance of alumina and a zirconia-toughened alumina (ZTA). The most commonly used method for assessing thermal shock resistance is to quench components, or specimens, from elevated temperatures into aqueous solutions and to measure the post-shock mechanical strength as a function of increasing ΔT, the temperature difference between the furnace and the solution. This procedure was followed in the present study and the AE and AU data were correlated with the strength measurements.

2. Experimental procedure

The two materials chosen to be investigated were a ZTA comprising a 99.5% Al_2O_3 plus 20 wt % ZrO_2 (stabilized with 3 mol % Y_2O_3), in the form of rectangular test bars of nominal dimensions $3 \times 3 \times 32$ mm, and a 99.1% Al_2O_3 fabricated into counterface rings. The latter was chosen in order to determine whether the acoustic techniques were capable of monitoring a component as well as test bars of simple geometry. The volume of the rings was 1374 mm^3 and was greater than that of the bars (288 mm^3). In addition to these materials, Si_3N_4, which has a much greater thermal shock resistance, was tested.

The thermal shock resistance was characterized for ΔT values up to 600 °C. The specimens were heated to the quench temperature, equilibrated, then rapidly quenched from a height of 10 cm into the quench medium of an aqueous solution of ethylene glycol at 20 °C.

An AE transducer of resonant frequency 150 kHz was positioned so that it was just in contact with the quench medium. The good acoustic coupling between

0022–2461/91 $03.00 + .12

the quench medium, the specimen and the transducer ensured that stress waves emanating from thermal stress induced microcracking in the specimen would propagate through the quench medium to the transducer. The signals from the transducer were analysed using commercially available AE equipment with facilities for ringdown counting, event counting, amplitude distributions and pulse width distributions. A total gain of 93 dB (preamplification 40 dB), a threshold of 25 dB and an envelope of 100 μs were used throughout the work. A schematic illustration of the AE system is given in Fig. 1.

The AU evaluation was undertaken using the AE system described above, in conjunction with a second transducer (pulser) connected to a pulsing unit capable of varying the amplitude and rate of the input pulses (stress waves) (Fig. 2). The pulse rate was approximately 1 Hz and readings were cumulated for 50 input pulses. The experiments were repeated for three different input amplitudes of 1, 4 and 7, specified on an arbitrary scale of up to 10, which was the maximum amplitude that could be generated.

The modulus of rupture of the bars of ZTA was measured in three-point bending in air at room temperature using a cross-head speed of 1 mm/min and a span to depth ratio of 8. The Al_2O_3 counterface rings were also tested in three-point bending and the fracture loads recorded.

Some post-shock structural observations were made. Dye penetrant testing was used to examine the microcrack morphology and the proportion of monoclinic zirconia at the surface (to a depth of about 20 μm) was determined by X-ray diffraction in accordance with the method proposed by Fillet *et al.* [6].

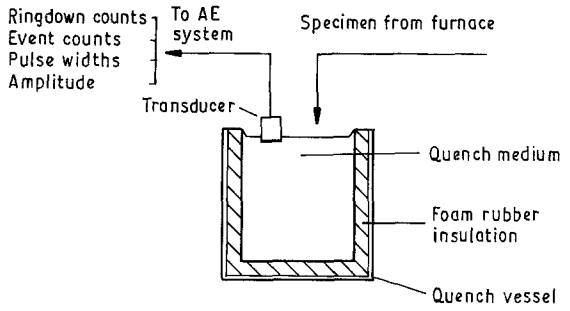

Figure 1 Schematic illustration of the experimental arrangement to monitor acoustic emission activity during thermal shock into an aqueous environment.

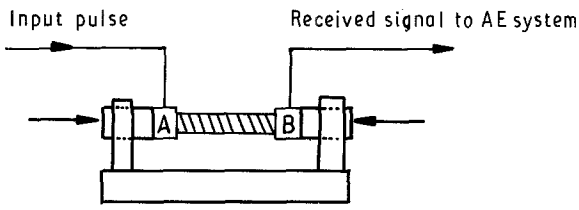

Figure 2 Schematic illustration of the experimental arrangement for post-thermal shock monitoring by acousto-ultrasonics. (▨ specimen; A, Pulsing transducer; B, receiving transducer; (→ ←) constant load spring.

3. Results

The results of the post-thermal shock strength measurements show some strength degradation at $\Delta T = 270\,^{\circ}C$ for the ZTA and only 23% of the initial strength by $\Delta T = 310\,^{\circ}C$ (Fig. 3). The strength degradation commenced at lower ΔT values for the alumina; there was a small loss in fracture load at $\Delta T = 180\,^{\circ}C$ and the retained strength was 35% of the as-received value by 270 °C.

The effect of ΔT on the AE count parameters, namely ringdown count and event count, was similar and hence only ringdown count data are presented here (Fig. 4). The data demonstrate that there is a sharp increase in the number of counts at $\Delta T = 180\,^{\circ}C$ for both alumina and ZTA. In contrast, the number of counts recorded for Si_3N_4 remained small over the full ΔT range employed in the investigation. At temperatures in excess of 180 °C, more ringdown and event counts were observed for the ZTA than the alumina. Only slight differences were found between the amplitude distributions for the alumina

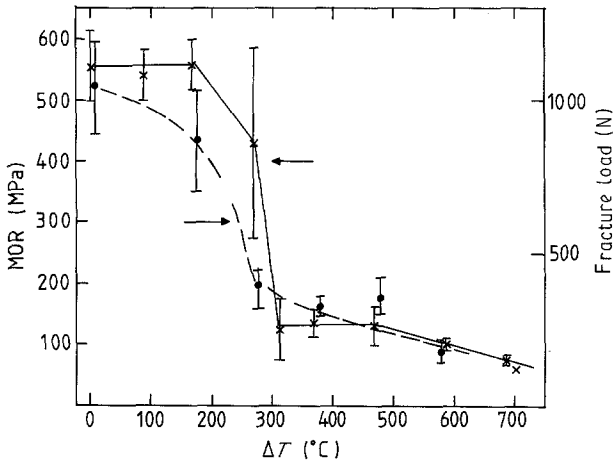

Figure 3 Strength degradation as a function of thermal shock treatment for ZTA (×) and alumina. Al_2O_3 (– ● –).

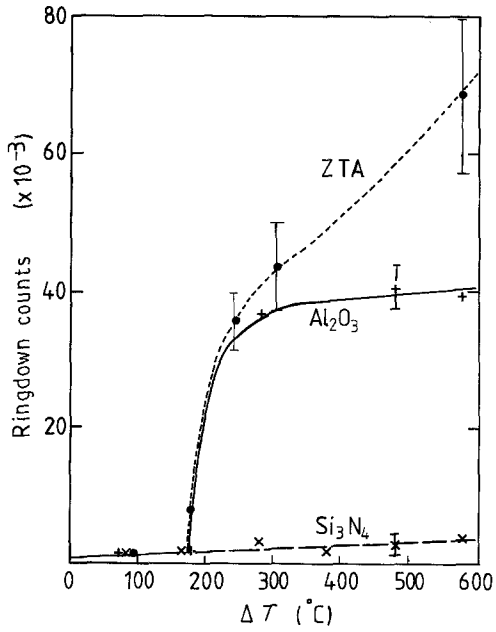

Figure 4 Ringdown counts from AE monitoring as a function of ΔT for ZTA, alumina and Si_3N_4.

and the ZTA. For both ceramics most of the emissions had amplitudes of less than 40 dB at all ΔT values, however, in the ΔT range 180–480 °C the main peak was centred around 25 dB whereas at higher temperatures the distribution was bimodal with an additional peak centred around 35 dB. The proportion of events with amplitudes exceeding that of the main peak(s) was greater for the ZTA, e.g. at $\Delta T = 380$ °C 50% of the events occurred after the main peak compared to 30% for alumina.

The acoustic response of the alumina and the ZTA during AU testing showed similar trends as a function of ΔT. As shown in Figs 5 and 6, the cumulative ringdown count for input amplitude of 1 exhibited a rapid decrease at 180 °C and 280 °C for ZTA and alumina, respectively, and thereafter remained constant. At higher input amplitudes, the same rapid decrease was observed but then the counts decreased more gradually with ΔT before reaching a constant value. It is worth noting that more counts were obtained from the alumina counterface rings than from the ZTA bars.

The plots of AU pulse width against ΔT showed similar features to those previously described for the ringdown count, although in the case of alumina tested at input amplitude of 7, a constant value was not reached at high ΔT (Figs 7 and 8). In contrast to the ringdown count and pulse width, there was no change in the amplitude, within experimental error, as ΔT increased for all three input amplitudes.

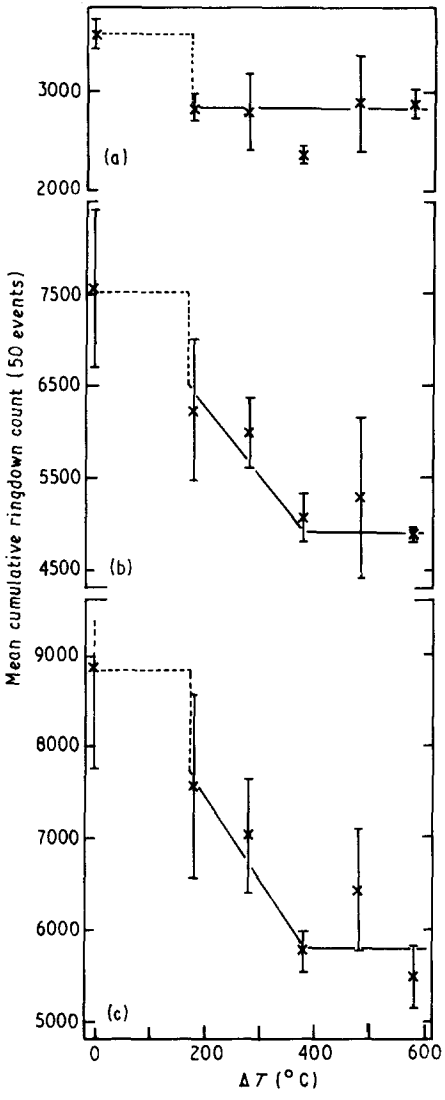

Figure 5 Cumulative ringdown count against ΔT for ZTA bars subjected to acousto-ultrasonic testing at input amplitudes of 1 (A), 4 (B) and 7 arbitrary units (C).

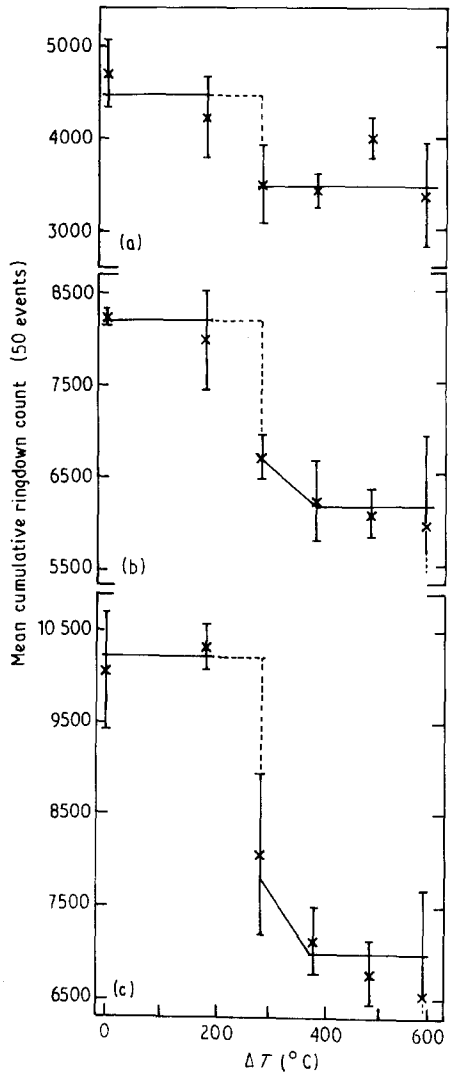

Figure 6 Cumulative ringdown count against ΔT for alumina counterface rings subjected to acousto-ultrasonic testing at input amplitudes of 1 (A), 4 (B) and 7 arbitrary units (C).

The dye penetrant testing revealed that at intermediate values of ΔT, irrespective of specimen composition or geometry, a network of fine microcracks developed at the surface, the density of which increased with increasing ΔT. At higher values of ΔT, i.e. $\Delta T > 400$ °C, the morphology changed and the high density of fine microcracks was replaced by fewer, but larger, microcracks. This change in morphology with ΔT is shown schematically in Fig. 9.

One of the most important microstructural features of ZTA is the proportion of the strengthening zirconia that is in the monoclinic condition. The X-ray diffraction results for the $3 \times 3 \times 32$ mm bars, on which all the other tests have been carried out, are presented in Fig. 10. This shows that the monoclinic content in the region of the surface increased with increasing ΔT to a maximum at $\Delta T = 400$ °C, beyond which it decreased until at 730 °C it had reached the same level as

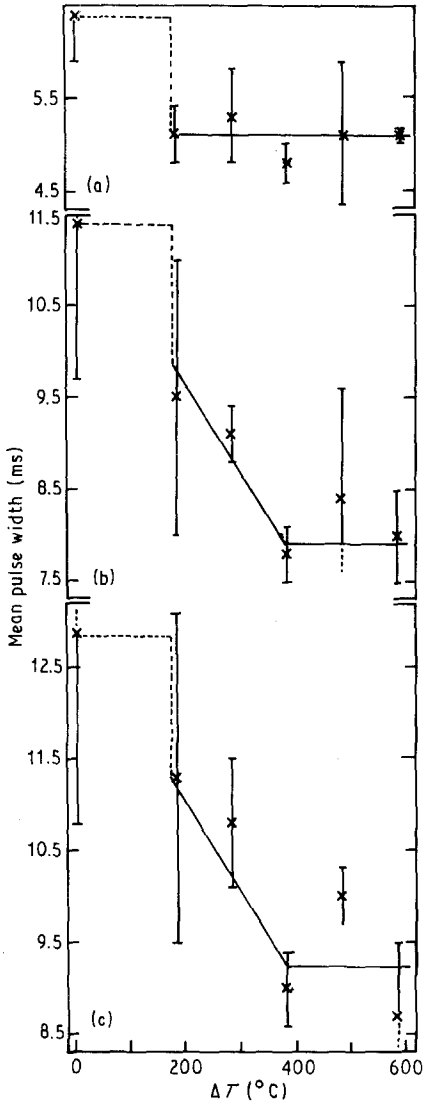

Figure 7 Pulse width against ΔT for ZTA bars subjected to acousto-ultrasonic testing at input amplitudes of 1 (A), 4 (B) and 7 arbitrary units (C).

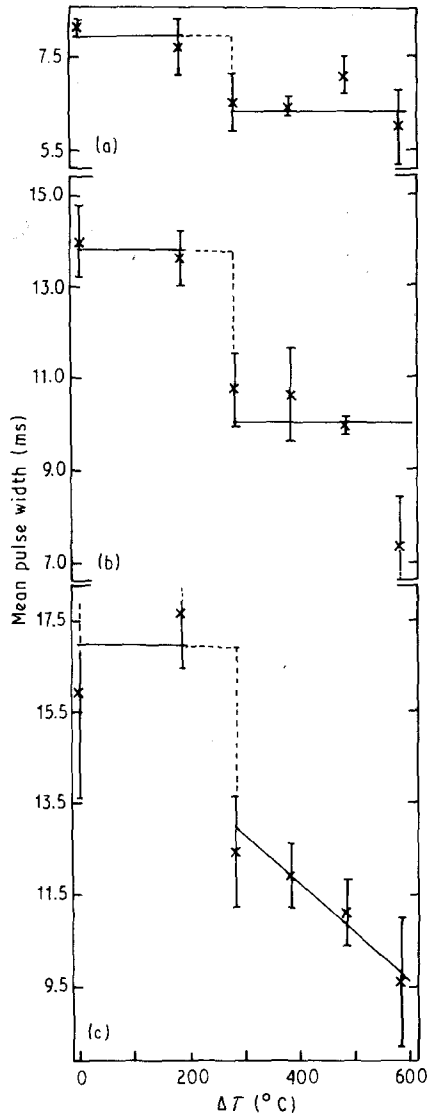

Figure 8 Pulse width against ΔT for alumina counterface rings subjected to acousto-ultrasonic testing at input amplitudes of 1 (A), 4 (B) and 7 arbitrary units (C).

in the as-received material. The experiment was repeated on larger ($7 \times 5 \times 50$ mm) bars and, as also shown in Fig. 10, the same trend with ΔT was found with the maximum occurring at a slightly lower ΔT of 280 °C.

4. Discussion

Comparison of the retained strength values of the ZTA with those for the alumina rings, and also with those for alumina spheres and bars from previous work [3], indicates that ZTA has the better thermal shock resistance. This is consistent with the growing evidence in the literature that a dispersion of second phase particles can enhance the thermal shock resistance of a ceramic [7]. Furthermore, the particles do not have to undergo a shear transformation and thus give transformation toughening to improve the thermal shock resistance. However, in the present case it is clear from the increase in the monoclinic content that some transformation toughening has taken place.

The ΔT dependence of the monoclinic content at the surface of the ZTA is a consequence of the changes in microcrack morphology. The point to note is that

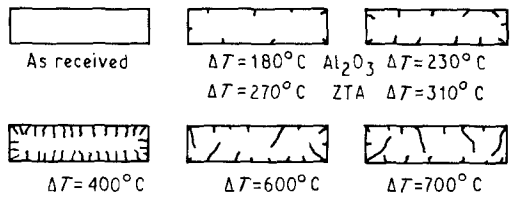

Figure 9 Change in crack morphology with increasing ΔT, showing a transition from a dense network of fine microcracks at low values of ΔT to fewer coarse microcracks at higher ΔTs, i.e. $\Delta T > 400$ °C.

the microcrack morphology changes at about $\Delta T = 400$ °C, which is the ΔT value at which the monoclinic content reaches its maximum. As the density of fine microcracks increases with increasing ΔT up to 400 °C, more of the zirconia particles are able to transform due to the removal of the matrix constraint in the vicinity of the cracks (Fig. 11b). However, above 400 °C the network of fine microcracks is replaced by a much smaller number of larger microcracks; thus the removal of the matrix constraint is more localized and fewer tetragonal particles undergo the transformation to the monoclinic as schematically illustrated in

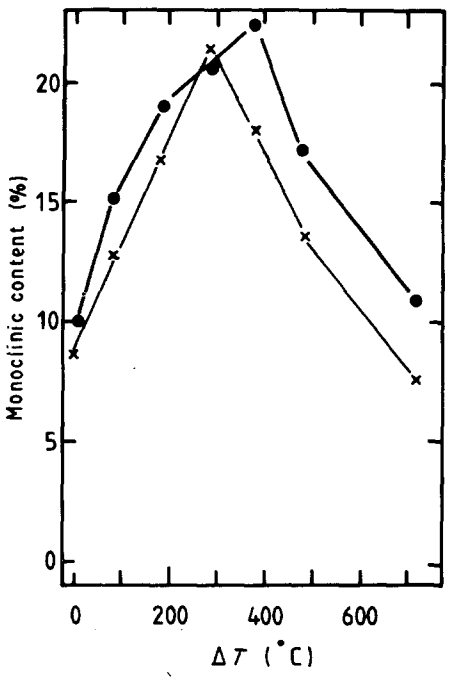

Figure 10 Percentage monoclinic phase as a function of ΔT for ZTA bars of small (●) $3 \times 3 \times 32$ mm^3; (×) $7 \times 5 \times 50$ mm^3 dimensions.

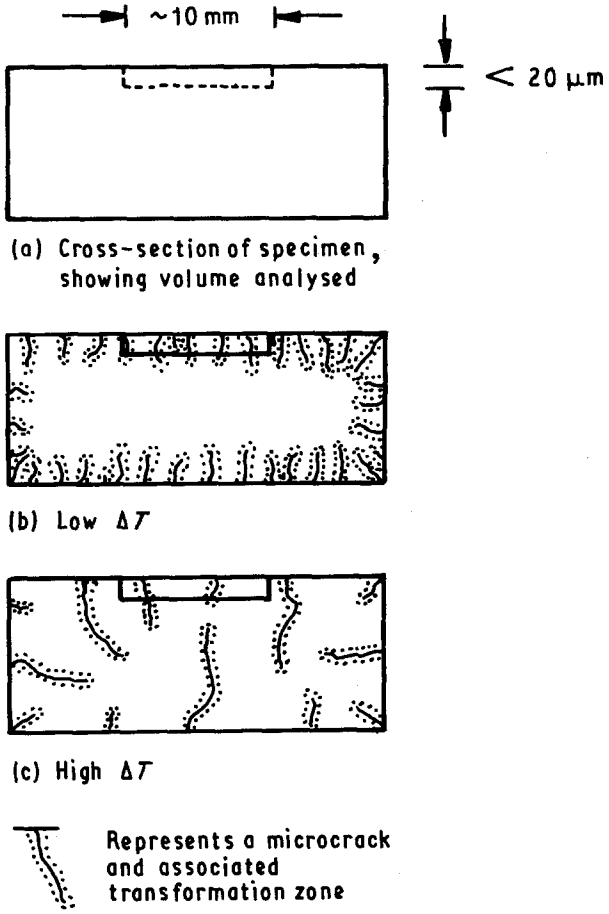

Figure 11 Schematic illustration of the influence that the change in crack morphology has on the extent of transformation to the monoclinic phase at the surface to a depth of about 20 μm.

Fig. 11c. It should be borne in mind that although the monoclinic content at the surface decreases at high ΔT values, the total volume transformed does not necessarily follow the same trend.

The negligible number of emissions detected for the Si_3N_4, which showed no evidence of microcracking under the thermal shock conditions used, establishes that spurious noise due to impact and bubbles was insignificant. The AE results given in Fig. 4 for alumina and ZTA demonstrate that the technique is capable of detecting the process of microcracking. ΔT for the onset of emissions coincided with that for a degradation in strength for alumina but was lower than that for a degradation in strength in the case of ZTA. It appears that ZTA can tolerate a small amount of thermally induced microcracking without compromising strength. Other than at $\Delta T = 180\,^{\circ}C$ and below, the ringdown and event counts were greater for ZTA. This is somewhat surprising as the volume of the ZTA bars was smaller than that of the alumina rings and, also, at a given ΔT, the extent of cracking was slightly less. This apparent discrepancy could be accounted for if the stress induced shear transformation in the ZTA contributed to the overall acoustic response. Certainly it is well documented that shear transformations, such as that in steels, produce elastic stress waves and therefore it is not surprising to find that AE has been used to monitor the tetragonal to monoclinic transformation in zirconia ceramics [8]. The greater proportion of higher amplitude events for the ZTA is also tentatively attributed to the same phenomenon.

The significance of the AE data is that it may be used to estimate retained strength from plots of counts, either event or ringdown, against strength. From plots such as that of Fig. 12, the number of counts which, if exceeded, would indicate structural damage to the component, could be specified. The limits that might be chosen from Fig. 12 are 10 000 and 15 000 counts for the alumina counterface rings and ZTA bars, respectively. Clearly an AE accept/reject procedure could be employed for monitoring the production of components and/or in-service behaviour.

The AU results of Figs 5–9 show that both ringdown count and the pulse width are suitable for monitoring thermal shock damage in alumina and ZTA. The reduction in the ringdown count and the pulse width at high ΔT values is consistent with the

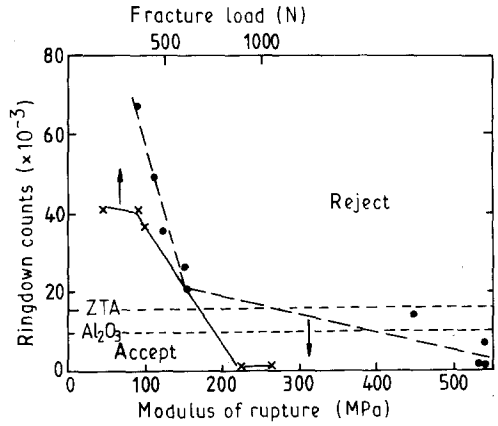

Figure 12 Plots of AE data for ZTA bars and alumina counterface rings which enable accept/reject criteria to be specified. (–●–) ZTA; (×) Al_2O_3.

elastic stress waves being scattered by the microcracks; increasing the porosity content of sintered glass and carbon-bonded carbon fibre composites has been shown to have the same effect on these AU parameters [5]. On the other hand, no changes were observed in the amplitude values with ΔT. However, this is attributed to the insensitivity of the equipment which employs a dB, and hence logarithmic, scale with a resolution of $\pm$ 1 dB for the amplitude measurements. Recent work on analysing waveforms using a personal computer has given reproducible and significant changes in the amplitude which were not detected on the dB scale.

The AU parameters indicate that some degradation has occurred at $\Delta T = 180\,^{\circ}C$ for the ZTA. This is in agreement with the AE results and confirms that some microcracking must have occurred without any measureable concomitant strength degradation. In the case of the alumina rings, the change in the AU parameters was observed, not at $\Delta T = 180\,^{\circ}C$, but at $\Delta T = 280\,^{\circ}C$ the next ΔT investigated. Both the AE and the strength measurement demonstrate that thermal shock damage commences at 180 °C; the reason for this discrepancy in the results is not known.

The smaller number of counts and the shorter pulse widths recorded for the ZTA in the as-received and shocked conditions compared to the corresponding conditions for the alumina may be a consequence of scattering by the zirconia particles, although the differences in specimen size and geometry may have also played a role. The absolute values of the ringdown count and the pulse width was, as expected, a function of the input amplitude, but in addition the percentage decrement in these parameters due to thermally induced damage was also dependent on the input amplitude (Table 1). The percentage decrement increased on increasing input amplitude from 1 to 4, and remained at the higher level for input amplitude 7. For a given input amplitude and material the changes in the ringdown count and the pulse width were within a few per cent of each other. Furthermore, similar percentage decrements were obtained from both materials, which suggest that the maximum damage was also similar. It is interesting to note that the constant value of the AU parameters observed in most cases at input amplitudes of 4 and 7, commenced at about $\Delta T = 400\,^{\circ}C$ and as such may be related to the change in crack morphology previously described.

As for the AE data, plots of AU parameter against retained strength may be constructed to yield accept/reject criteria. The plot for ZTA (Fig. 13) gives

TABLE I The percentage decrement in the cumulative ringdown count (RC) and the pulse width (PW) for the ZTA bars and the alumina rings after thermal shock treatment at $\Delta T = 580\,^{\circ}C$.

Material	AU Parameter	Decrement (%)		
		Input 1	Input 4	Input 7
ZTA	RC	19	37	34
ZTA	PW	20	31	30
Alumina	RC	22	27	31
Alumina	PW	21	28	32

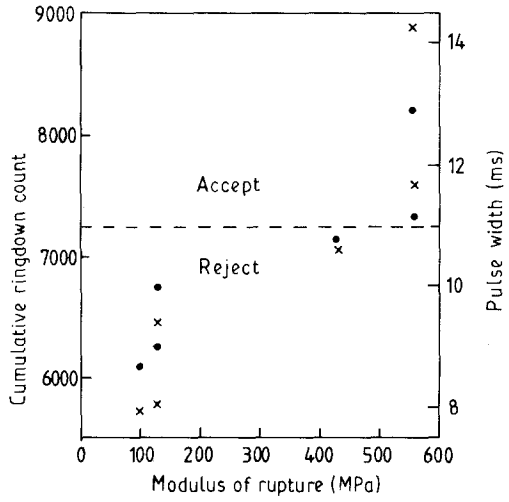

Figure 13 Plots of ringdown count and pulse width from AU testing against retained strength which enable accept/reject criteria to be specified for ZTA bars. (×) Ringdown; (●) pulse width.

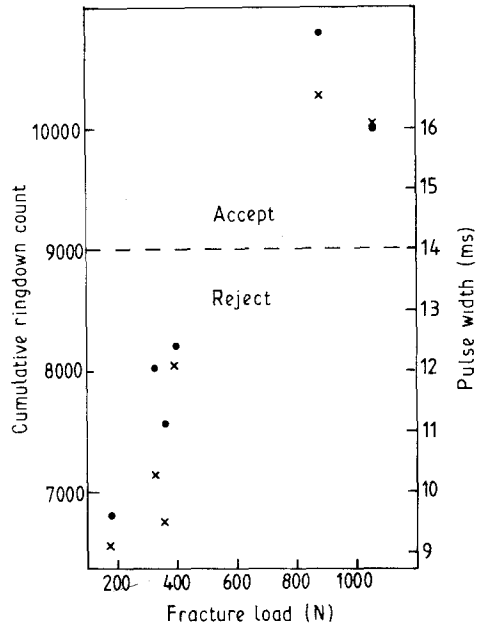

Figure 14 Plots of ringdown count and pulse width from AU testing against retained strength which enable accept/reject criteria to be specified for alumina counterface rings. (×) ringdown; (●) pulse width.

limits of 7250 and 11.0 ms for the ringdown count and pulse width, respectively. The corresponding limits for the alumina are 9000 counts and 14.0 ms (Fig. 14). However, it must be remembered that these limits will only apply for components of the shape and size used in this investigation. At this stage of development of the technique, because of complications due to phenomena such as resonance and the wave guide effect, it is necessary to produce calibration plots similar to those shown in Figs 13 and 14 for each material/component combination.

5. Conclusions

The retained strength measurements indicate that the thermal shock resistance of ZTA is better than that of alumina. Acoustic emission is found to be capable of

monitoring thermally induced microcracking as it takes place. Acousto-ultrasonics is also capable of monitoring thermally induced microcracking during post-shock testing. In general, there was good agreement between the retained strength data and the results from the acoustic techniques. Both acoustic emission and acousto-ultrasonic results could therefore be used for accept/reject criteria.

Acknowledgements

The authors would like to thank Morgan Matroc Ltd, which supplied the materials and also supported the research through a SERC CASE studentship.

References

1. B. J. DALGLEISH, P. L. PRATT, R. D. RAWLINGS and A. FAKHR, *Mater. Sci. & Engng* **45** (1980) 9.
2. K. E. AEBERLI and R. D. RAWLINGS, *J. Mater. Sci. Letts.* **2** (1983) 215.
3. I. THOMPSON and R. D. RAWLINGS, *Institute of Ceramics* **42** (1988) 15.
4. A. DE, K. K. PHANI and S. KUMAR, *J. Mater. Sci. Letts.* **6** (1987) 17.
5. A. O. B. ADUDA and R. D. RAWLINGS, Presented at 7th CIMTEC World Ceramic Congress, Montecatini Terme, Italy (1990) Proc. to be published by Elsevier.
6. R. FILLIT, J. HOMERIN, H. BRUYAS and F. THEVENOT, *J. Mater. Sci.* **22** (1987) 3566.
7. G. FANTOZZI, *Silicates Industriels*, **5** (1988) 67.
8. D. R. CLARKE and A. ARORA, *Amer. Ceram. Soc. Advances in Ceram.* **12** (1984) 54.

Received 30 August
and accepted 29 October 1990